Title
Suction-Induced Hardening Effects on the Shear Modulus of Unsaturated Silt

Journal
International Journal of Geomechanics, 16(6)

ISSN
1532-3641

Authors
Khosravi, Ali
Salam, Sajjad
McCartney, John S
et al.

Publication Date
2016-12-01

DOI
10.1061/(asce)gm.1943-5622.0000614

Peer reviewed

Suction-induced Hardening Effects on the Shear Modulus of Unsaturated Silt

Ali Khosravi, Ph.D.
Assistant Professor
Sharif University of Technology, Department of Civil Engineering
Tehran, Iran; khosravi@sharif.edu

Sajjad Salam
Undergraduate Student
Sharif University of Technology, Department of Civil Engineering
Tehran, Iran; sajjad_salam@sharif.edu

John S. McCartney, Ph.D., P.E.
Associate Professor
University of California San Diego, Dept. of Structural Engineering
9500 Gilman Dr. La Jolla, CA 92093-0085; mccartney@ucsd.edu

Ali Dadashi
Graduate Student
Sharif University of Technology, Department of Civil Engineering
Tehran, Iran; ali.dadashi86@gmail.com

ABSTRACT

The small strain shear modulus G_{max} is a key material parameter in modeling the behavior of soils subjected to dynamic loading. Recent experimental results indicate seasonal weather interaction with near-surface soils causes G_{max} to change by up to an order of magnitude in some climates, with a hysteretic response upon drying and wetting. The increase in G_{max} during drying and the stiffer response during subsequent wetting have been postulated to be due to plastic hardening during drying. In order to further understand this behavior, a series of isotropic compression tests were performed on compacted silt specimens at different values of matric suction to evaluate changes in the preconsolidation stress with suction. The G_{max} values obtained from a previous study on this silt matched well with a model using a hardening parameter independently derived from the isotropic compression tests as well as the parameters of the soil-water retention curve (SWRC). The model shows an increase in G_{max} during drying from an initially saturated condition that is directly related to the increase in preconsolidation stress with suction, and the trends in G_{max} follow transitions in the shape of the SWRC. The hardening parameter from these tests was also suitable to model the greater values of G_{max} encountered during rewetting of the soil. The role of the preconsolidation stress in the model confirms that changes in G_{max} correspond to elasto-plastic hardening mechanisms during drying rather than solely to changes in matric suction.

KEYWORDS: Unsaturated soils, small strain shear modulus, plastic hardening, resonant column, isotropic compression, degree of saturation

INTRODUCTION

The dynamic shear modulus of soils, G, is a material property widely used in evaluating wave propagation through soil layers and predicting ground deformations and the dynamic response of earth structures under cyclic, dynamic, or earthquake loading. Experimental studies on silts and clays illustrated that the following soil characteristics tend to have a significant effect on dynamic shear modulus of soils: the mean effective stress p', void ratio e, degree of saturation S_r, stress history (i.e., the overconsolidation ratio, OCR), maximum principal stress difference, soil grain characteristics (mineralogy), and strain amplitude (Hardin and Black 1969; Hardin and Drnevich 1972; Hardin 1978). For dynamic loading-induced strains less than 10^{-4}%, the shear modulus is constant (i.e., it does not depend on strain), is referred to as the maximum or small-strain shear modulus G_{max}, and represents the elastic response of the soil (Hardin and Black 1969; Hardin and Drnevich 1972; Hardin 1978).

Improvements in experimental soil mechanics led to the development of different empirical relationships between G_{max} and some relevant parameters of soils in their water saturated or dry conditions (Hardin and Black 1968, 1969; Seed and Idriss 1970; Hardin and Drnevich 1972; Hardin 1978; Vucetic and Dobry 1991; Stokoe *et al.* 1999). However, little attention was given to the stiffness variations in unsaturated soils due to environmental interactions and the effect of complex phenomena taking place during drying and wetting. Some of the relevant aspects differentiating unsaturated soils from dry and saturated soils are the stress state (Khalili et al. 2004; Lu and Likos 2006; Nuth and Laloui 2008), suction-induced hardening behavior (Alonso et al. 1990), and hydraulic hysteresis (Wheeler et al. 2003, Tamagnini 2004). In regions of aeration above the water table within man-made or natural soil structures, the soil may be subjected to variation in stiffness because of the seasonal interactions with the atmosphere, leading to repeated cycles of infiltration and evaporation, referred to as hydraulic hysteresis. The seasonal wetting and drying of unsaturated soils in these systems imply that the stiffness of the soils may change during operation (McCartney and Khosravi 2012), leading to varying resilience to strain development during dynamic loading (Birgisson et al. 2007). Due to these mechanisms, a more complex model to capture trends in the small strain shear modulus of unsaturated soils with these different phenomena may be needed than those used for dry or saturated soils.

Although it is well understood that unsaturated stress state variables, mean net stress, p_n, and matric suction, ψ, play an important role in the mechanical behavior of soils in their unsaturated state (Bishop 1959; Fredlund and Morgenstern 1977), approaches to consider the impact of hydraulic hysteresis and degree of saturation in G_{max} have only recently been considered (Ng et al. 2009; Khosravi and McCartney 2011; Khosravi and McCartney 2012; Heitor et al. 2014). Khosravi and McCartney (2011) utilized a Stokoe-type resonant column test that was modified using the axis translation technique (Hilf 1956) to evaluate the dependency of the small strain shear modulus of a low plasticity soil to unsaturated stress state and hydraulic hysteresis. The testing approach included a fixed-free resonant column test setup adopted with the axis translation technique for suction control, and a flow pump for degree of saturation control. Similar to the degree of saturation measurements, results of this study revealed a hysteresis behavior in G_{max} values along the drying and wetting paths of the soil-water retention curve (SWRC). Based on G_{max} values measured on the primary drying path, the compacted specimens experienced a nonlinear increase in G_{max} with matric suction increase, followed by a decreasing path during subsequent re-wetting. However, the original G_{max} value was not fully recovered after the re-wetting with the values of G_{max} being consistently higher than those obtained during drying. Results showing similar trends to those observed by Khosravi and McCartney (2011) were also reported by Khosravi and McCartney (2009), Ng et al. (2009), Khosravi et al. (2010), and Heitor et al. (2014).

Khosravi and McCartney (2012) characterized the hysteresis behavior of G_{max} as a result of drying-induced hardening which was not fully recovered during wetting and developed a new hydro-mechanical model for the G_{max} of unsaturated soils. The new model incorporated elasto-plastic constitutive relationships which integrate the effects of mean effective stress and hardening due to either plastic changes in volume or changes in the degree of saturation. Specifically, the concept of double hardening for unsaturated soils (Wheeler *et al.* 2003; Tamagnini 2004) was adapted to consider the impact of hydraulic hysteresis on G_{max} of low plasticity soils as follows:

$$G_{\max} = AP_a \left[\frac{p_c'_0}{p_n} \exp\left(\frac{\Delta e^p}{\lambda - \kappa} \right) \right]^K \left[\frac{p_n}{p'} \exp\left(b[S_{e0} - S_e] \right) \right]^{K'} \left(\frac{p'}{P_a} \right)^n \quad (1)$$

where P_a is the atmospheric pressure, A and n are stress dependency parameters, p_c' is the mean apparent preconsolidation stress (i.e., the mean yield stress), p' is the mean effective stress, p_n is the net stress, Δe^p is a plastic change in void ratio, λ and κ are the slopes of the virgin compression and the elastic rebound curves, respectively, K' and K are hardening constants, $p_c'_0$ is the initial the mean apparent preconsolidation stress, b is referred to as the double-hardening parameter which governs the rate of change in p_c' caused by changes in the degree of saturation, S_{e0} is the initial effective saturation, and S_e is the effective saturation which is defined as:

$$S_e = \frac{S_r - S_{r,res}}{1 - S_{r,res}} \quad (2)$$

In Eq. 2, S_r and $S_{r,res}$ are the values of S_r at current and residual saturation conditions. The proposed model was then validated against experimental data obtained from the resonant column tests on low plasticity materials. Although the model provided a good fit to the measured G_{max}, the hypothesis behind this study (dependency of the G_{max} values to the suction-induced hardening) was only investigated theoretically and the hardening parameters in Eq. 1 were defined by fitting the model to the experimental G_{max} data using least-squares regression.

In the work presented herein, an experimental study has been performed to investigate the evolution of the yield surface of unsaturated silt specimens following drying and wetting paths. These results were then used to independently define key parameters that are needed to predict the variation in G_{max} for unsaturated soils during hydraulic hysteresis using the model proposed by Khosravi and McCartney (2012). In this regard, the evolution of the yield surface during hydraulic hysteresis was investigated using a suction-controlled triaxial test device. High confining pressure magnitudes up to 1700 kPa were applied using a high pressure hydraulic pump. In addition, a fixed-free Stokoe-type resonant column (RC) test device with suction-saturation control was also utilized to measure changes in G_{max} during hydraulic hysteresis. Specifically, a flow pump originally used in permeameter tests to measure the hydraulic conductivity of saturated and unsaturated soils was operated with suction-feedback control to establish equilibrium conditions for G_{max} evaluation. Results of this testing program were then used to obtain parameters that are required to describe the hardening mechanism due to suction and evaluate hardening-induced changes of G_{max} along different paths of the SWRC.

MATERIAL AND SPECIMEN PREPARATION

Tested material

The tested material is a silt obtained from the Bonny dam whose hydraulic properties have been widely investigated (Bicalho et al. 2007; Khosravi and McCartney 2011; Khosravi and McCartney 2012; Khosravi et al. 2012; Alsherif and McCartney 2014). The soil was selected as it retains water over a wide range of suction values, and may show different behaviors when wetted and dried at different effective stress values. The amount of suction-induced volume change in Bonny silt was observed to be relatively small (Khosravi and McCartney 2012). As a result, the information gained through their use facilitated interpretation of the impact of unsaturated stress states. Bonny silt is classified as ML in accordance with the Unified Soil Classification System (USCS) (ASTM D2488-00) with some relevant index properties summarized in Table 1. Based on the results of the flexible-wall permeameter and the vapor flow techniques presented by Khosravi and McCartney (2012) and Alsherif and McCartney (2014), an air entry suction value of 10 kPa and a residual saturation value of 0.05 can be assumed for statically-compacted silt specimens with an initial void ratio of 0.69.

Specimen preparation

Laboratory tests to assess the effect of suction-induced hardening on the small strain shear modulus of low plasticity soils were performed on a group of specimens which were completely remolded and prepared in the laboratory. To prepare the tested specimens, the soil particles were initially screened through a No. 40 sieve and then oven-dried at a temperature of 110°C. After a period of 24 hours, dried soil was uniformly mixed with de-aired distilled water at an average gravimetric moisture content of 14% and then placed in a sealed plastic bag for 24 hours. After that, the soil was statically compacted in a cylindrical mold having a diameter of 35.1 mm and a height of 70 mm to an initial void ratio, *e*, of 0.69. The static compaction was performed following the undercompaction procedure described by Ladd (1978) in three lifts and the interfaces between the successive layers were scarified for better interpenetration with the subsequent layer. At the end of the compaction, the specimen was removed from the mold, its weight and dimensions were measured, and then quickly placed in the triaxial cell in order to minimize any water loss.

EXPERIMENTAL SETUPS

Isotopic compression test setup

In the current study, a conventional triaxial cell modified with the Axis Translation technique (Hilf 1956) was used to outline the effects of suction on the behavior of soils at large strain. The new setup was designed to accommodate the application of high confining pressure magnitudes using a high pressure hydraulic pump which is capable of applying pressures up to 1700 kPa (Figure 1). In this device, the bottom platen of the triaxial setup was modified to accommodate a high air-entry (HAE) ceramic disc to control suction in the specimen. To prevent stress concentrations beneath the disc, a traditional coarse porous stone was embedded in the bottom platen underneath the disc.

Water flow from the specimen during the application of increments of mean net stress and matric suction was measured using visual observation of water levels in graduated burettes connected to the water drainage lines from the specimen and the chamber. Measurements from these systems are used to obtain changes in the degree of saturation and the volume of the specimen during loading. Possible sources of error with this method of water/specimen volume measurements are expansion/contraction of the triaxial chamber, burettes and the pressure line tubing, which can considerably affect the experimental measurements. To account for these sources of error, the volume measurements during a given test were corrected using the results of a series of careful calibration tests performed on an aluminum cylinder under the same laboratory conditions and pressure ranges applied to the soils to measure changes in volume due to the compliance of the cell and tubing under different pressure levels. The tests were performed under a backpressure of 300 kPa, which was applied to the bottom of the specimen during testing to minimize the possibility for diffused air to come out of solution. This simplifies the measurement of water flow to and from the specimen during wetting or drying, respectively.

Resonant column test device

A fixed-free Stokoe-type resonant column test device with suction-saturation control was used to monitor the shear waves transmitted through the specimens and measure the hardening-induced changes in G_{max} during hydraulic hysteresis. In this regard, a swept sine signal with constant amplitude was supplied to a non-contact electromagnetic drive plate resting atop the specimen. The first-mode of resonance of the tested specimen was then interpreted from the angular frequency response and was used in the equation of Richart et al. (1970) to calculate the shear wave velocity of the soil specimen. G_{max} was then calculated from V_s as follows:

$$G_{\max} = \rho V_s^2 \tag{3}$$

where ρ is the mass density of the soil specimen.

In this test device, the axis translation technique (Hilf 1956) was implemented to control suction in the specimen using a high air-entry (HAE) ceramic disc, with an air-entry suction value of 100 kPa. The top surface of the HAE disc was lightly inscribed to promote coupling with the soil and a high conductivity, texturized Teflon water distribution disc was embedded within the bottom platen to ensure a uniform distribution of water to the overlying HAE ceramic disc. The value of S_r of the specimen was controlled using a flow pump system connected to the bottom platen of the resonant column device and a differential pressure transducer incorporated into a suction-feedback control loop was implemented to reach different equilibrium values of ψ and S_r in the soil specimen. In this test setup, change in height of the specimen during testing was inferred from the measurements of a non-contact proximity sensor mounted on top of the drive plate. The height measurements obtained from the proximity sensor readings were used to estimate the change in void ratio by assuming that the soil deforms isotropically. This assumption overestimates the void ratio measurements of compacted soil specimens, which will behave in an anisotropic manner. However, the small changes in void ratio had a relatively minor effect on the calculated value of S_r and G_{max} (Khosravi and McCartney 2011).

EXPERIMENTAL PROCEDURES

The testing program in this study consists of two different sets of testing: isotropic compression tests on soil specimens under constant matric suction values, and resonant column tests performed on soil specimens subjected to successive cycles of drying and wetting. The specimens were compacted to a target void ratio of 0.69 and were tested following the stress paths presented in Figure 2.

Isotropic compression test procedure

The experimental program to examine the effect of soil suction on hardening/softening behavior of unsaturated soils comprises a series of isotropic, high-pressure, compression tests at different suction levels through the drying and wetting paths of the SWRC. After the preparation of the soil specimen within the triaxial setup, the specimen was placed under backpressure by increasing the chamber and the pore pressures in stages to values of 335 and 300 kPa, respectively. After equalization under these stresses, Skempton's B-value parameter was checked to evaluate the saturation of the tested specimens, and was found to be 0.98 or higher for the tests presented in this paper.

Once the saturation stage ended, the desired matric suction was introduced at the boundaries of the specimen by lowering (increasing upon wetting) the backpressure applied to the bottom of the specimen while keeping the air pressure constant at the top. Water outflow from the specimen during the application of matric suction was measured through the graduated burettes, and sufficient time was permitted to reach hydraulic equilibrium. In this study, “equilibrium” was defined as being reached when there was no change in water outflow for at least 10 hours. After reaching hydraulic equilibrium, the isotropic compression test was initiated by increasing the cell pressure in stages to achieve mean net stresses as high as of 1400 kPa, while keeping the pore pressures constant.

At the end of the test, the specimens were removed from the cell and their dimensions, weight, and water content were measured. This process was then repeated for specimens of different densities at different values of matric suction along the drying and wetting paths of the SWRC to define the relationship between specific volume, matric suction, and the mean net stress for the tested material.

Resonant column test procedure

The test procedure used with the modified resonant column test device consists of four stages of saturation, compression, suction equilibrium, and dynamic testing on specimens of different initial densities. During the saturation stage, the backpressure saturation technique (Lowe and Johnson 1960) was used to dissolve the pore air in the pore water and increase the saturation of the tested specimen. In this regard, the chamber and pore water pressures were simultaneously increased in stages to values of 520 kPa and 450 kPa, respectively, maintaining the effective stress equal to 70 kPa. After saturation, the specimens were isotropically compressed to the desired effective stress by increasing the cell pressure while keeping pore water pressure constant (Compression stage). After ensuring that the volume of the specimen is constant, the value of G_{max} corresponding to saturated conditions was measured by performing a resonant column test on the specimen under drained conditions at the desired mean net stress.

After this point, the flow pump was used to withdraw water from the bottom of the specimen (through the HAE disc) at a constant rate until a target suction value is obtained. The flow pump was guided using a suction-feedback control loop to reach different equilibrium values of suction and degree of saturation in the soil specimen. After reaching hydraulic equilibrium, a resonant column test was performed to measure G_{max} of the soil specimen in an unsaturated state. This process was repeated to measure multiple points on the SWRC and define the relationship between G_{max}, ψ, and S_r. After defining the drying path of the SWRC, the wetting process was initiated by reversing the direction of movement of the pump piston to supply water to the specimen in controlled increments. More details about the resonant column test procedure can be found in Khosravi (2011), Khosravi and McCartney (2011) and Khosravi and McCartney (2012).

RESULTS

Isotropic compression test results

Five isotropic compression tests (one under saturated condition, three along the drying path of the SWRC at suctions of 10, 31 and 55, and one along the wetting path at a suction of 45 wetted from an initial matric suction of 71 kPa) were carried out on specimens molded with a constant void ratio of 0.69 with the aim of identifying the LC surface of the compacted silt for suctions along drying and wetting paths of the SWRC. For each test, the changes in void ratio of the soil specimens were inferred from the measured water volume withdrawn from the chamber minus the known machine deflection of the triaxial cell obtained from the results of the calibration tests. The relationships between void ratio and mean net stress for the five tests are shown in Figure 3(a). Similarly, the change in water volume withdrawn from the specimen was used to measure changes in the degree of saturation, S_r. The degree of saturation versus mean net stress is shown in Figure 3(b).

During an isotropic compression test on unsaturated soil, due to collapse of the voids in the pore space, all of the specimens exhibited a decreasing volume as the mean net stress was increased (Figure 3a). However, those soil specimens that were subjected to higher levels of suction exhibited a smaller amount of compression under a given applied mean net stress and their corresponding void ratio measurements were consistently higher than those in low suction testing. This has the effect of shifting the compression curve to the right, indicating a hardening response in compacted specimens as a result of suction increase. Also, as shown in Figure 3(b), during isotropic compression, the soil specimens experienced an increase in their corresponding degree of saturation with a mean net stress increase. The rate of increase was different, greater in those with a lower initial degree of saturation.

For an isotropic stress state, the process of hardening experienced by the compacted soil is associated with a loading collapse yield curve in the p'-ψ space. The shape of the yield curve can be obtained from the compression curves presented in Figure 3(a) and their corresponding yield points (defined as the mean preconsolidation stress, p_c') along the drying and wetting cycles of the SWRC. In this regard, the results presented in Figure 3(a) were reinterpreted in terms of the mean effective stress, p' in Figure 4 and then the p_c' values of the curves were defined as the intersection of the lines extended from straight-line portions of the elastic rebound and virgin compression curves. The effective stress, p', in this plot was defined using the concept of suction stress proposed by Lu and Likos (2006) as follows:

$$p' = p_n + p_s \quad (4)$$

where p' is the mean effective stress, p_n is the net stress, and p_s is the mean suction stress. Suction stress is a stress variable which describes the contribution of matric suction to the effective stress and can be determined from a closed form equation proposed by Lu et al. (2010) as follows:

$$p_s = \frac{S_r - S_{r,res}}{1 - S_{r,res}}\psi \qquad (5)$$

where S_r and $S_{r,res}$ are the values of S_r at current and residual saturation conditions. Similar methods were used by Wheeler et al. (2003) and Khosravi and McCartney (2012) to identify the yield points in isotropic compression tests.

The variation of p_c' with matric suction together with the corresponding SWRC are presented in Figure 5. As shown in Figure 5, for the range of suction less than the air entry value, only small changes in p_c' are measured. However, for suctions greater than the air entry value, the changes in ψ lead to significant changes in S_r and consequently changes in p_c' happen at a greater rate. During wetting, a hysteretic behavior in p_c' is noted and the results indicate higher values of p_c' compared to those obtained during drying.

Resonant column test results

The results from the resonant column tests at various values of mean net stress are shown in Figure 6. The SWRC of the tested specimens in terms of the effective saturation is shown in Figure 6(a), the soil specimen volume changes with the applied matric suction are shown in Figure 6(b), and the values of G_{max} measured after reaching equilibrium during each stage of the drying and wetting tests are shown in Figure 6(c). The effective saturation values in Figure 6(a) were obtained by converting the values of S_r from the experimental measurements using Eq. 2 with a value of $S_{r,res}$ equal to 0.05.

The results presented in Figure 6 suggest that the mean net stress has great influence on water retention ability of the tested specimens and their corresponding degree of saturation measurements. Under high mean net stresses, the soil specimens may have a new pore size distribution (Ng and Pang 2000; Khosravi and McCartney 2012) that has the effect of shifting the SWRC to the right (i.e., higher air entry suction) from its location at low mean net stresses. During wetting, a higher energy is required to displace air trapped in the larger pores of the soil specimens under lower mean net stresses. As a result, the soil specimens will absorb less water during wetting and their hydraulic hysteresis loop will be larger compared to those subjected to higher values of mean net stress.

In contrast to the S_r measurements, only minor changes in void ratio were recorded along the drying and wetting paths of the SWRC. The void ratio vs. matric suction data shown in Figure 6(b) indicates that the specimens stayed on the elastic unloading-reloading curve throughout the test. As a result, the effect of volume changes on the measured SWRC and G_{max} relationships for the tested specimens were ignored.

A comparison of changes in G_{max} in Figure 6(c) indicates two distinct regimes in the variation in G_{max} along the drying path of the SWRC. In the first regime, the value of G_{max} initially experienced a slight increase in magnitude with increasing ψ at suction values below the air entry value. This regime is typically associated with small variations in the degree of saturation. In the second regime, the value of G_{max} followed a nonlinear trend at higher suctions, where the changes in suction on the drying path led to significant changes in the degree of saturation. During wetting, the soil specimen initially absorbed a small amount of water along a scanning path. Accordingly, only a slight reduction in G_{max} with decreasing ψ was recorded. Between the water-entry value and the air-expulsion value, the soil started to absorb more water along the wetting path of the SWRC leading to a greater decrease in G_{max} with a decrease in ψ.

The effect of subsequent drying and wetting on the small strain shear modulus was also examined by performing a series of resonant column tests on a specimen with an initial void ratio of 0.69 along subsequent cycles of drying and wetting. In this regard, after achieving the full saturation of the tested specimen using the backpressure technique, the soil specimen was initially dried to a suction value of 31 kPa along the main drying path of the SWRC. After that, the direction of the flow pump was reversed and the applied suction was decreased in stages to a value of 20 kPa to produce the first scanning curve of the test. At each point of suction equilibrium, a resonant column test was performed and the value of G_{max} of the soil specimens was measured. The specimen was then re-dried and a similar procedure was followed at suction values of 41 and 61 kPa for simulating three full cycles of drying and wetting. The stress state conditions are presented in Figure 7 and the results are shown in Figure 8. The variations of G_{max} measured after reaching equilibrium with matric suction is presented in Figure 8(a) and the SWRCs of the tested specimens are shown in Figure 8(b). Results presented in this figure revealed a slight hysteresis in the G_{max} measurements along the scanning curves of the SWRC, with a larger loop along the second loop where more significant changes in S_r happened with changing matric suction. However, in both cases, the value of G_{max} was recovered once the main drying path was reached. Similar observations were reported by Heitor et al. (2014).

ANALYSIS

In early studies on G_{max} of saturated and dry soils (Hardin 1978), hardening effects were considered through the overconsolidation ratio, OCR, defined as:

$$OCR = \frac{p_c'}{p'} \quad (6)$$

where p_c' is the mean apparent preconsolidation stress and p' is the mean effective stress. In an unsaturated soil during hydraulic hysteresis, different distributions of water are expected in a soil specimen depending on whether the soil is undergoing drying or wetting. As a consequence, even though the suction may have the same magnitude at some point during drying or wetting, different values of p_c' and p' may be possible for this suction value during hydraulic hysteresis (Wheeler et al. 2003; Tamagnini 2004; Khalili and Zargarbashi 2010). Accordingly, the *OCR* is not sufficient to represent hardening effects in unsaturated soils and the relationship for G_{max} during hydraulic hysteresis should be defined with the values of p_c' and p' considered separately.

Khosravi and McCartney (2012) described the hardening effects associated with changes in degree of saturation using an expression for p_c' as follows:

$$\frac{dp_c'}{p_c'} = -\frac{de^p}{(\lambda - \kappa)} - bdS_e \quad (7)$$

where de^p is a plastic change in void ratio, λ is the slope of the virgin compression curve, and κ is the slope of the elastic rebound curve, b is referred to as the double-hardening parameter, and S_e is the effective saturation which is defined using Eq. 2. Eq. 7 is very similar to that defined by Tamagnini (2004) except that S_e is incorporated instead of S_r. The first term on the right side of Eq. 7 describes the evolution of the yield surface (i.e., hardening) produced by plastic changes in volume during isotropic loading and the second term describes the evolution of the yield surface resulting from changes in S_e. For the compacted specimens of Bonny silt, the compression curves exhibited relatively little volume change for the range of stress variables (matric suction and mean net stress) used in the resonant column testing (Figure 6). Accordingly, the value of de^p in Eq. 7 can be assumed to be zero and the equation of p_c' can be re-written as follows:

$$\frac{dp_c'}{p_c'} = -bdS_e \quad (8)$$

The advantage of using Eq. 8 to predict the value of p_c' is that it only requires a single parameter b, and permits direct incorporation of S_e values from the SWRCs at different mean net stresses. Because it incorporates the value of S_e instead of suction, different values upon wetting and drying can be obtained. The hardening parameter, b, which controls the rate of change in p_c'

with changes in S_e can be determined by comparing the values of p_c' estimated using Eq. 8 with those obtained from the isotropic compression tests (Figure 5). Based on the experimental measurements, a value of b equal to 0.93 was found to best represent the change in preconsolidation stress with matric suction.

In the current study, the value of b obtained from the isotropic compression tests was used in Eq. 8 to predict the variation of p_c' for the range of suctions and net stresses used in resonant column testing (Figure 2). The predicted trends in p_c' were then used to explain the hardening behavior in the values of G_{max} measured in the resonant column tests. The values of mean preconsolidation stress obtained from Eq. 8 as a function of matric suction are presented in Figure 9(a). The values of G_{max} obtained from the resonant column tests are also presented in Figure 9(b) for the comparison purposes.

Results of the mean preconsolidation stress presented in Figure 9(a) confirm that the preconsolidation stress increases with suction during drying, then remains at a higher value during wetting. Results also indicate higher values of p_c' at lower values of mean net stress. A comparison of the trends in p_c' with the values of G_{max} measured in the resonant column tests indicated that the G_{max} values of the compacted specimens followed an S-shaped curve during drying and wetting complying with the S-shape of the p_c' curve. Along the drying path of the SWRC, the soil specimen experienced a drying-induced hardening and consequently, the measured p_c' followed an increasing path with suction increase. These changes in p_c' resulted in an increase in the G_{max} measurements during drying. During wetting, the developed stiffness along the drying path was not fully recovered and a hysteresis behavior was observed in G_{max} measurements with values measured along the wetting path greater than those measured during drying. Referring to the trends in p_c' and G_{max} measurements, it may be concluded that changes of p_c' as a result of flooding or emptying of voids with water, are much more important than the suction, ψ, in producing changes in the small strain shear modulus of compacted soil at an unsaturated state.

The hardening behavior observed in the isotropic compression tests was also linked to the hardening behavior in the values of G_{max} measured in the resonant column tests by using the value of b inferred from the results of isotropic compression tests to predict the changes in G_{max} during hydraulic hysteresis using the model of Khosravi and McCartney (2012) (Eq. 1). The trends in G_{max} predicted using Eq. 1 with those measured in the resonant column test are presented in Figure 10 in terms of the mean effective stress, p'. In this figure, the parameters required to predict the evolution of G_{max} during hydraulic hysteresis were defined through definition of the SWRC and compression curves, and through parameter fitting to this specific soil. Specifically, the values of S_e were obtained from the experimental measurements (Figure 4), and the value of K was defined using empirical guidance from Hardin (1978) for this type of soil (K = 0.05). The values of A and n were defined by fitting a curve to the values of G_{max} measured under saturated conditions (zero suction) and K' was obtained from the G_{max} measurements during subsequent wetting at different mean net stresses using least squares minimization. The effective stress, p' in this plot was defined using Eqs. 4 and 5 with a value of $S_{r,res}$ of 0.05. With these parameters, the model predictions shown in Figure 10 were observed to be consistent with the values of G_{max} measured in the resonant column tests. The model also showed the same trend due to the hardening effect caused by dying and wetting of the soil.

CONCLUSION

A testing program was presented in this paper to represent the impact of suction induced hardening on the dynamic shear modulus of unsaturated, compacted soils. Specifically, a series of resonant column tests were performed on compacted soil specimens to measure the values of small strain shear modulus under successive cycles of drying and wetting, and isotropic compression tests were utilized to characterize the evolution of the yield surface with matric suction changes and obtain the hardening parameters of the tested specimens.

The results presented in this study indicate that the hardening of soil caused by drying plays the most important role in the dynamic response of unsaturated soils at small strains. Based on the results of isotropic compression tests on the specimens with an initial void ratio of 0.69, the mean preconsolidation stress of the statically-compacted Bonny silt specimens varied from 720 to 1080 kPa for matric suctions ranging from 0 to 55 kPa. However, its value only decreased to a value of 1110 kPa upon re-wetting to a suction value of 45 kPa from an initial matric suction of 71 kPa. As a result of this hardening behavior, hysteresis behavior was observed in G_{max} measurements during drying and wetting. Along the drying path of the SWRC, the measured G_{max} followed an increasing path with suction increase. Upon rewetting, a stiffer response than that along the drying path was observed and greater magnitudes of G_{max} were measured.

The model proposed by Khosravi and McCartney (2012) found to be suitable for the characterization of the behavior of G_{max} under different values of mean net stress and hydraulic hysteresis, using model parameters defined independently from the SWRC, compression curve, and the relationship between G_{max} and effective stress for saturated soils. This observation confirms the importance of understanding the role of suction-induced hardening in modeling the impact of hydraulic hysteresis on the dynamic properties of unsaturated soils.

ACKNOWLEDGEMENT

The authors would like to thank Amin Gheibi and Mehrzad Rahimi, the graduate students of Civil Engineering Department at Sharif University of Technology for their assistance in performing the isotropic compression tests.

REFERENCES

Alonso, E.E., Gens, A., and Josa, A. (1990). "A constitutive model for partially saturated soils." *Géotechnique*. 40(3), 405-430.

Alsherif, N. A., & McCartney, J.S. (2014). "Effective stress in unsaturated silt at low degrees of saturation." *Vadose Zone Journal*, *13*(5), 1-13.

Bicalho, K.V., Znidarčić, D. and Ko, H.-Y. (2011). "One-dimensional flow infiltration through a compacted fine grained soil." *Soils and Foundations*. 51(2), 287-295.

Birgisson, B., Ovik, J., and Newcomb, D.E. (2007). "Analytical predictions of seasonal variations in flexible pavements: Minnesota road research project site." *Transportation Research Record*. 1730, 81-90.

Bishop, A.W. (1959). "The principle of effective stress." *Teknisk Ukeblad I Samarbeide Med Teknikk. Oslo*, Norway, 106(39), 859-863.

Fredlund D.G., Morgenstern, N.R. (1977). "Stress state variables for unsaturated soils." *Journal of Soil Mechanics and Foundation Division*. 103(5), 447–466.

Hardin, B.O. and Black, W.L. (1968). "Vibration modulus of normally consolidated clay." *Journal of the Soil Mechanics and Foundations Division*. 94(SM2), 353–369.

Hardin, B.O. and Black, W.L. (1969). "Vibration modulus of normally consolidated clay; Closure." *Journal of the Soil Mechanics and Foundations Division*. 95(SM6), 1531–1537.

Hardin, B.O. (1978). "The nature of stress strain behavior of soils." *Earthquake Engineering and Soil Dynamics*. June 19-21, Pasadena, California. ASCE. Vol. 1, 3–90.

Hardin B.O. and Drnevich, V.P. (1972). “Shear modulus and damping in soils: Measurement and parameter effects.” *Journal of the Soil Mechanics and Foundation Engineering Division*. 98(SM6), 603-624.

Heitor, A., Indraratna, B., & Rujikiatkamjorn, C. (2014). “Aspects related to the small strain shear modulus behaviour of compacted soils subjected to wetting and drying.” In *Proc. Geo-Congress 2014: Geo-characterization and Modeling for Sustainability*, ASCE, 1433-1442.

Hilf, J.W. (1956). An Investigation of Pore-Water Pressure in Compacted Cohesive Soils. Technical Memorandum No. 654, United State Department of the Interior Bureau of Reclamation, Design and Construction Division, Denver, Colorado, USA.

Khalili, N., Geiser, F., Blight, E. (2004). “Effective stress in unsaturated soils: Review with new evidence.” *International Journal of Geomechanics*. 4(2), 115-126.

Khalili, N., Zargarbashi, S. (2010). “Influence of hydraulic hysteresis on effective stress in unsaturated soils.” *Géotechnique*. 60(9), 729-734.

Khosravi, A. and McCartney, J.S. (2009). “Impact of stress state on the dynamic shear moduli of unsaturated, compacted Soils.” *Proceedings of the 4th Asia Pacific Conference on Unsaturated Soils*. Newcastle, Australia. Nov. 23-25. pp. 1-6. (CD-ROM).

Khosravi, A., Ghayoomi, M., McCartney, J.S., and Ko, H.Y. (2010). “Impact of effective stress on the dynamic shear modulus of unsaturated sand.” *GeoFlorida: Advances in Analysis, Modeling & Design*. ASCE, 199, 410-419.

Khosravi, A., and McCartney, J.S. (2011). “Resonant column test for unsaturated soils with suction-saturation control.” *ASTM Geotechnical Testing Journal*. *34*(6), 730-739.

Khosravi, A., and McCartney, J.S. (2012). “Impact of hydraulic hysteresis on the small-strain shear modulus of low plasticity soils.” *Journal of Geotechnical and Geoenvironmental Engineering*. 138(11), 1326-1333.

Ladd, R.S. (1978). “Preparing test specimens using under compaction.” *Geotechnical Testing Journal*. 1(1), 16–23.

Lowe, J. III and Johnson, T. C., “Use of back pressure to increase degree of saturation of triaxial test specimens.” In *Proc. Res. Conf. Shear Strength of Cohesive Soils*, ASCE, Boulder, Co, 1960, pp. 819-836.

Lu, N. and Likos, W.J. (2006). “Suction stress characteristic curve for unsaturated soil.” *Journal of Geotechnical and Geoenvironmental Engineering*. 132(2), 131-142.

Lu, N., Godt, J., and Wu, D., (2010). “A closed-form equation for effective stress in unsaturated soil.” *Water Resources Research*. 46(W05515), 1-14.

McCartney, J.S. and Khosravi, A. (2013). “Field monitoring system for suction and temperature profiles under pavements.” ASCE Journal of Performance of Constructed Facilities. 27(6), 818-825.

Ng, C.W.W., Xu, J. and Yung, S.Y. (2009). “Effects of imbibition-drainage and stress ratio on anisotropic stiffness of an unsaturated soil at very small strains.” *Canadian Geotechnical Journal*, 46(9), 1062-1076.

Ng, C.W.W. and Pang, Y.W. (2000). “Experimental investigations of the soil-water characteristics of a volcanic soil.” *Canadian Geotechnical Journal*. 37(6), 1252-1264.

Nuth, M. and Laloui, M. (2008). “Effective stress concept in unsaturated soils: Clarification and validation of a unified framework.” *International Journal of Numerical and Analytical Methods in Geomechanics*. 32, 771-801.

Richart, F. E., Jr., Hall, J., and Woods, R.D., (1970). Vibrations of Soils and Foundations. Prentice Hall, Englewood Cliffs, NJ.

Seed, H.B. and Idriss, I.M. (1970). Soil Moduli and Damping Factors for Dynamic Response Analyses. Earthquake Engineering Research Center, University of California at Berkeley, Report EERC-70/10.

Stokoe, K. H., II, Darendeli, M.B., Andrus, R.D., Brown, L.T. (1999). “Dynamic soil properties: Laboratory, field and correlation studies.” In *Proc. 2nd Int. Conf. on Earthquake Geotechnical Engineering*, Lisbon, Portugal. Vol. 3. 35 pg.

Tamagnini, R. (2004). “An extended Cam-clay model for unsaturated soils with hydraulic hysteresis.” *Géotechnique*. 54(3), 223–228

Vucetic, M. and Dobry, R. (1991). “Effect of soil plasticity on cyclic response.” *Journal of Geotechnical Engineering*. 117(1), 89-107.

Wheeler, S.J., Sharma, R.S., and Buisson, M.S.R. (2003). “Coupling of hysteresis and stress–strain behaviour in unsaturated soil.” *Géotechnique*. 53(1), 41–54.

LIST OF TABLES AND FIGURES

Table 1: Geotechnical parameters of Bonny silt

Fig. 1: Schematic of the modified triaxial cell to outline the effects of matric suction on the isotropic compression behavior of unsaturated soils

Fig. 2: Stress path used in the different testing programs: (a) Isotropic compression tests; (b) Resonant column tests

Fig. 3: Results of isotropic compression tests in terms of mean net stress: (a) Change in void ratio; (b) Change in degree of saturation

Fig. 4: Results of isotropic compression tests in terms of mean effective stress, p'

Fig. 5: Variation of p_c' with matric suction (LC yield curve) together with the corresponding SWRC

Fig. 6: Results of the resonant column tests for silt specimens with an initial void ratio of 0.69 at various values of mean net stress: (a) SWRC of the tested specimens in terms of the effective saturation; (b) Changes in the void ratio of the soil specimens with matric suction;(c) Values of G_{max} measured after reaching equilibrium during each stage of the drying and wetting tests

Fig. 7: Stress paths followed to assess the effect of subsequent cycles of drying and wetting on the G_{max} measurements of unsaturated compacted soils

Fig. 8: Hysteretic behavior during wetting and drying along the primary and scanning paths: (a) SWRC; (b) G_{max}

Fig. 9: Hardening behavior of the compacted silt specimen under different mean net stress during hydraulic hysteresis: (a) Changes in p_c' in terms of ψ, and; (b) Changes in G_{max} in terms of ψ

Fig. 10: Relationships between G_{max} and mean effective stress during hydraulic hysteresis predicted using hardening parameters from the compression tests and defined experimentally from resonant column tests

Table 1
Click here to download high resolution image

Parameter	Value	
D_{10}	<0.0013	mm
D_{30}	0.022	mm
D_{50}	0.039	mm
Pass. No. 200 Sieve, d_{200}	83.9	%
Clay Frac. (<2 μm), d_c	14	%
USCS	ML	
Specific Gravity, G_s		
Liquid Limit, LL	25	
Plasticity Index, PI	4	
Activity, A	29	
Maximum Dry Unit Weight, γ_d	16.3	kN/m^3
Optimum Water Content, w_{opt}	13.6	%
Compresion Index, C_c	0.04	
Recompression Index, C_r	2.8	%
Drained Friction Angle, ϕ'	29°	
Air Entry Suction, ψ	10	kPa
Residual Degree of Saturation, $S_{r,res}$	0.05	

Figure 1
Click here to download high resolution image

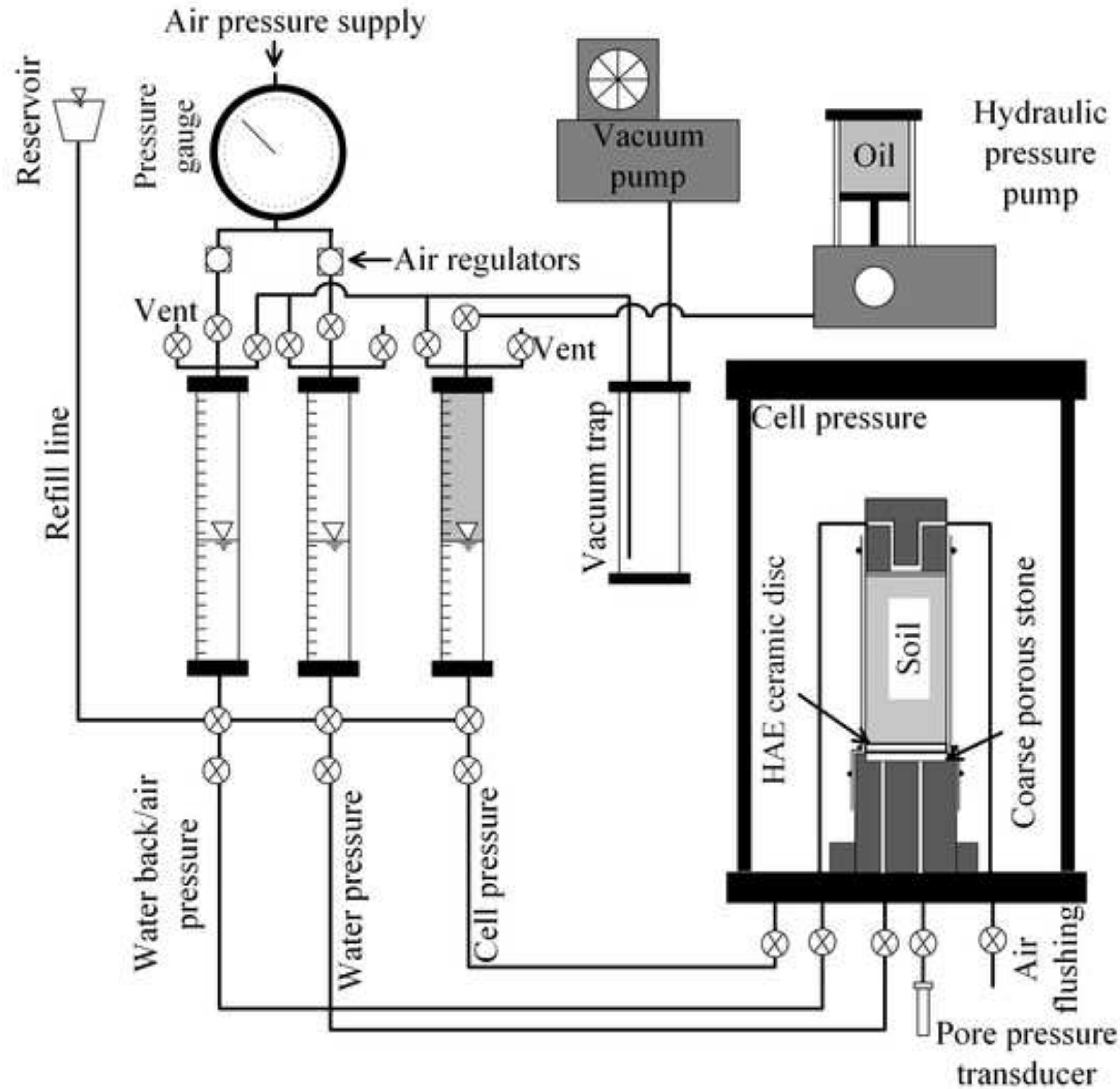

Figure 2
Click here to download high resolution image

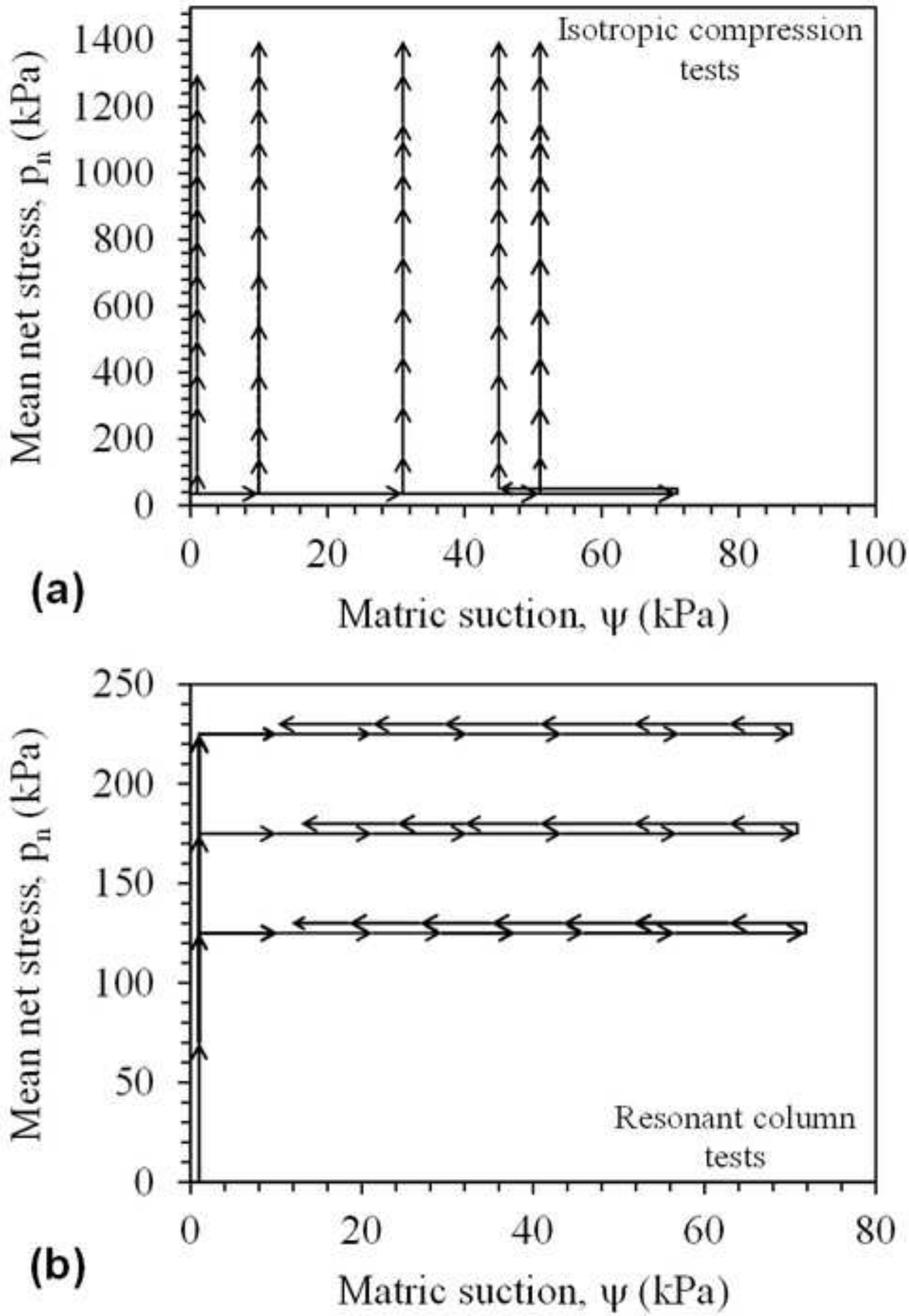

Figure 3
Click here to download high resolution image

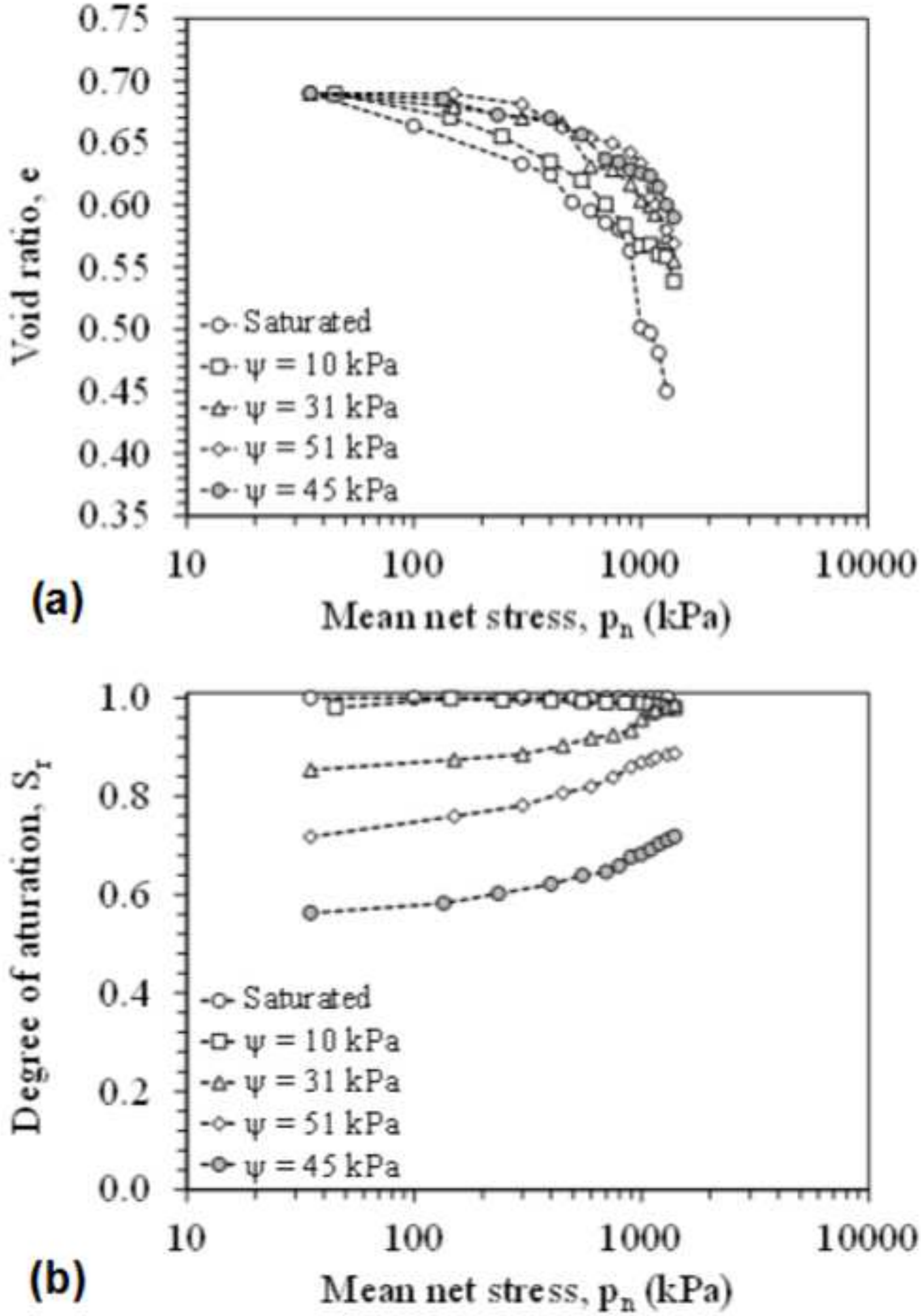

Figure 4

Click here to download high resolution image

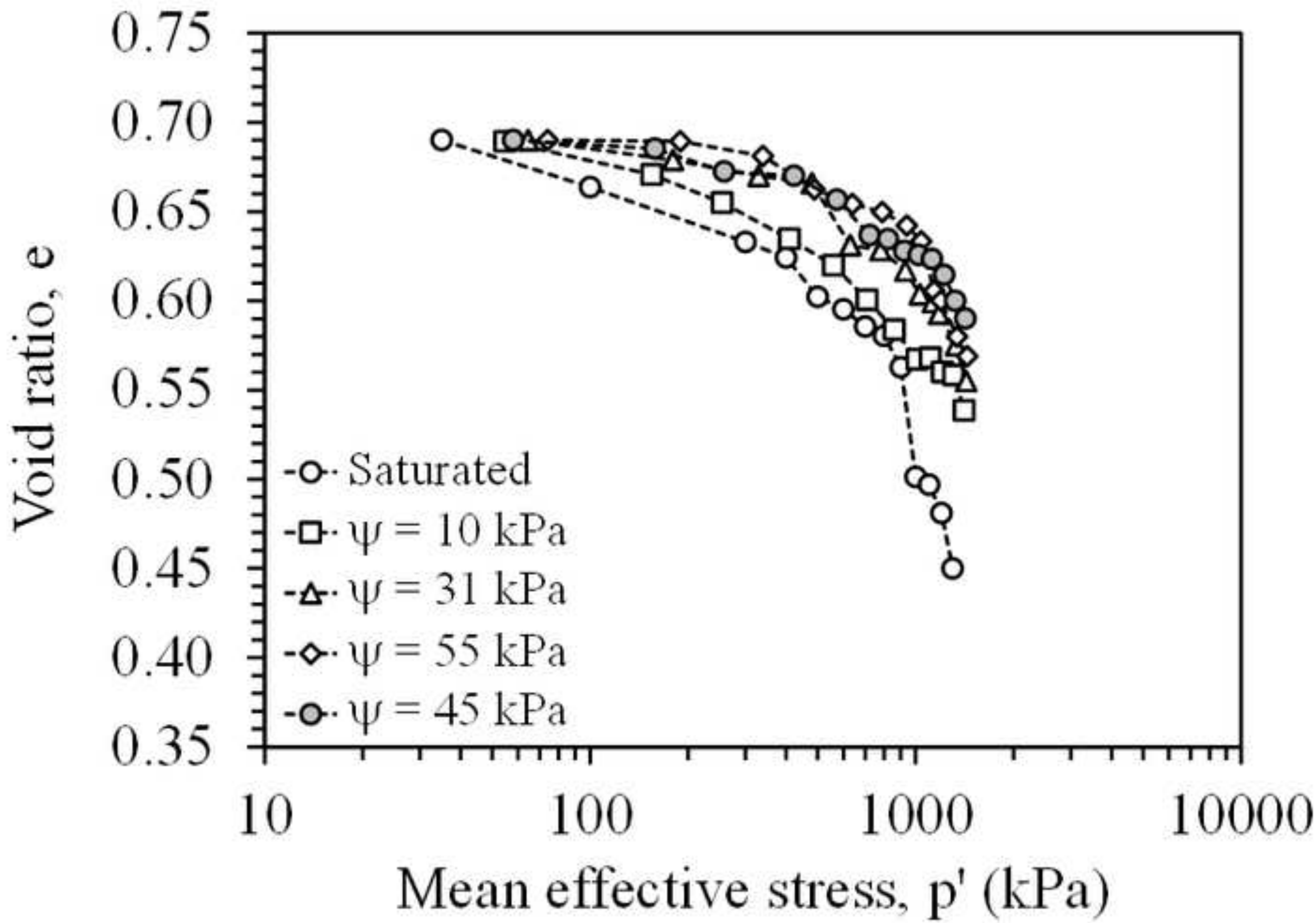

Figure 5
Click here to download high resolution image

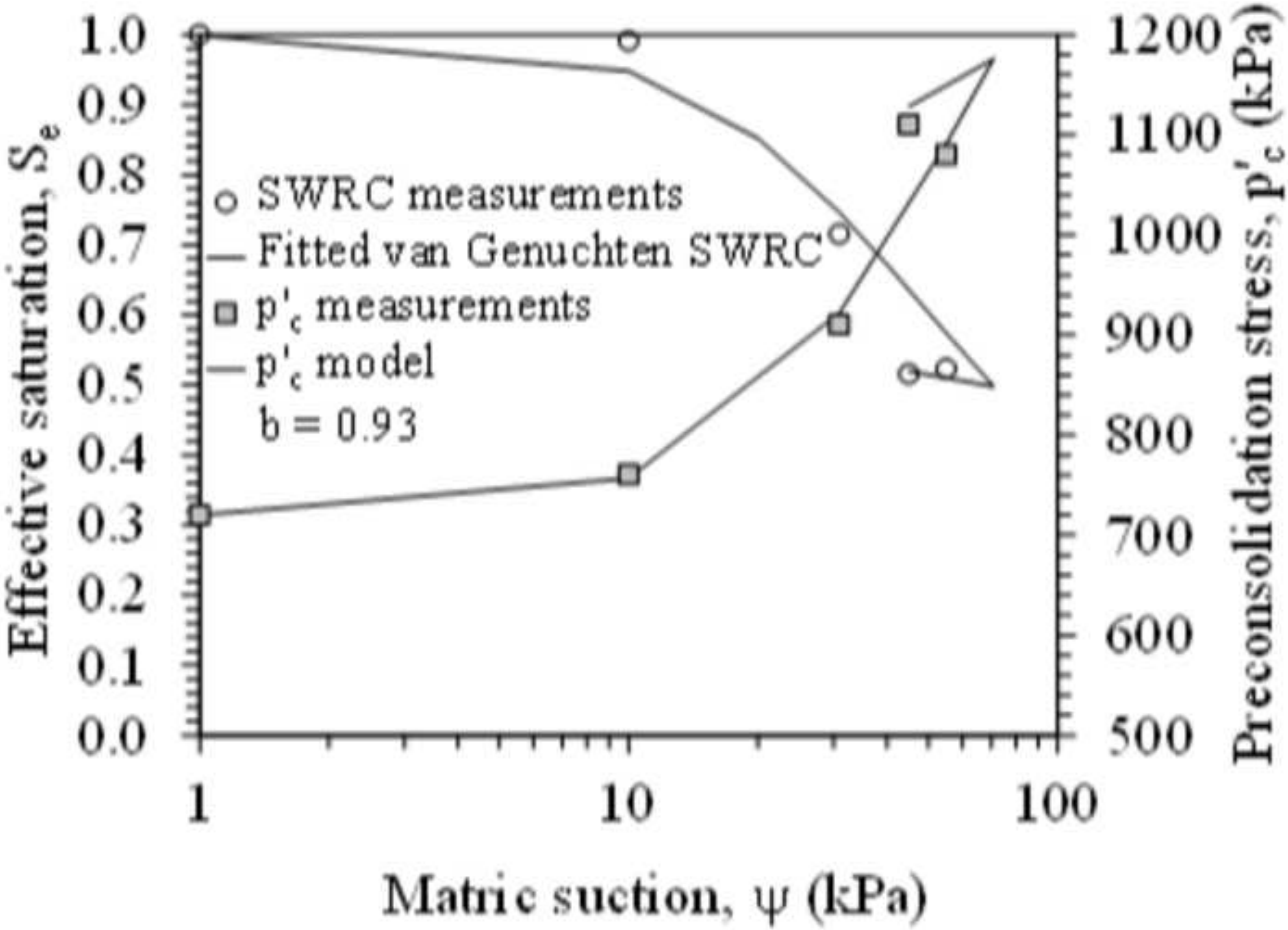

Figure 6
Click here to download high resolution image

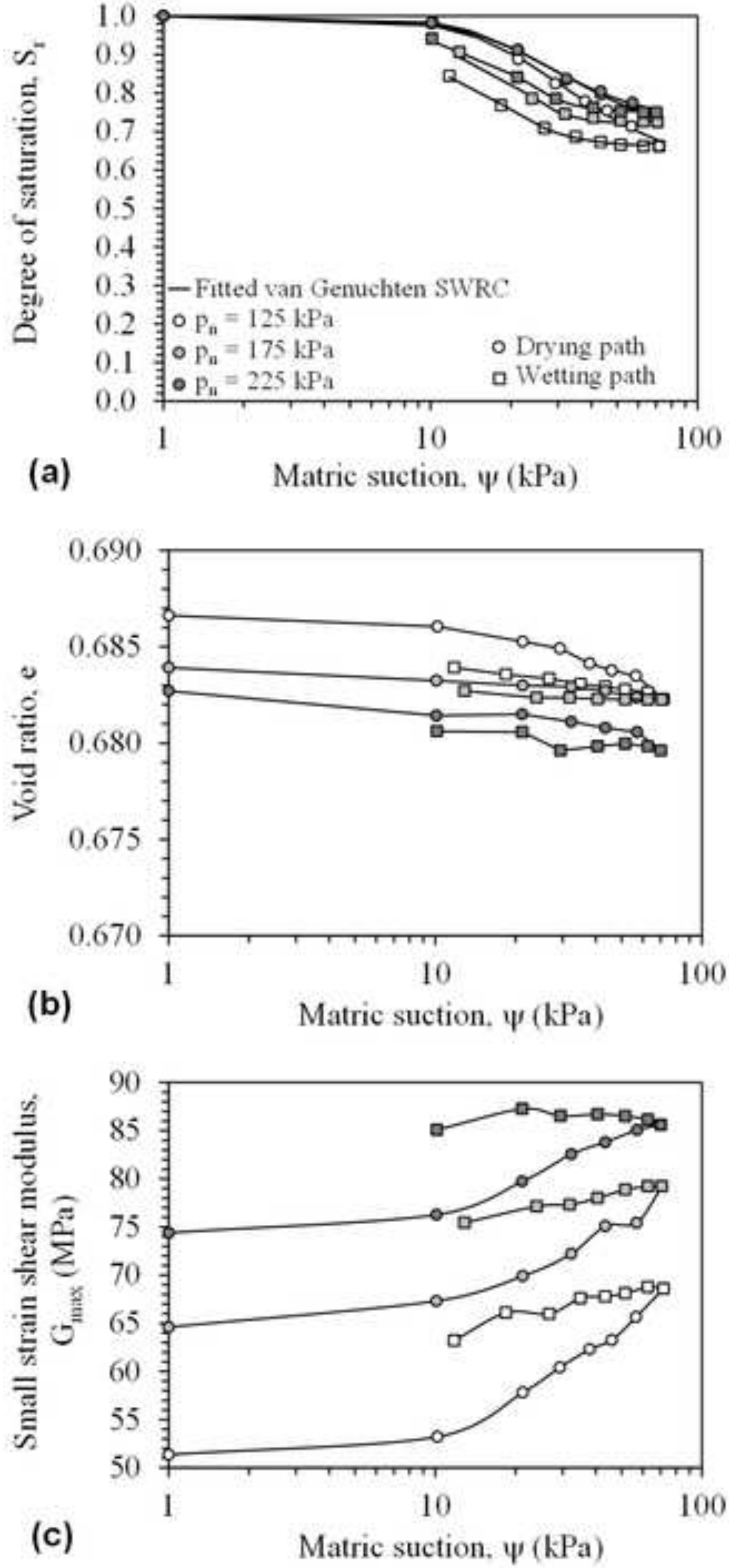

Figure 7
Click here to download high resolution image

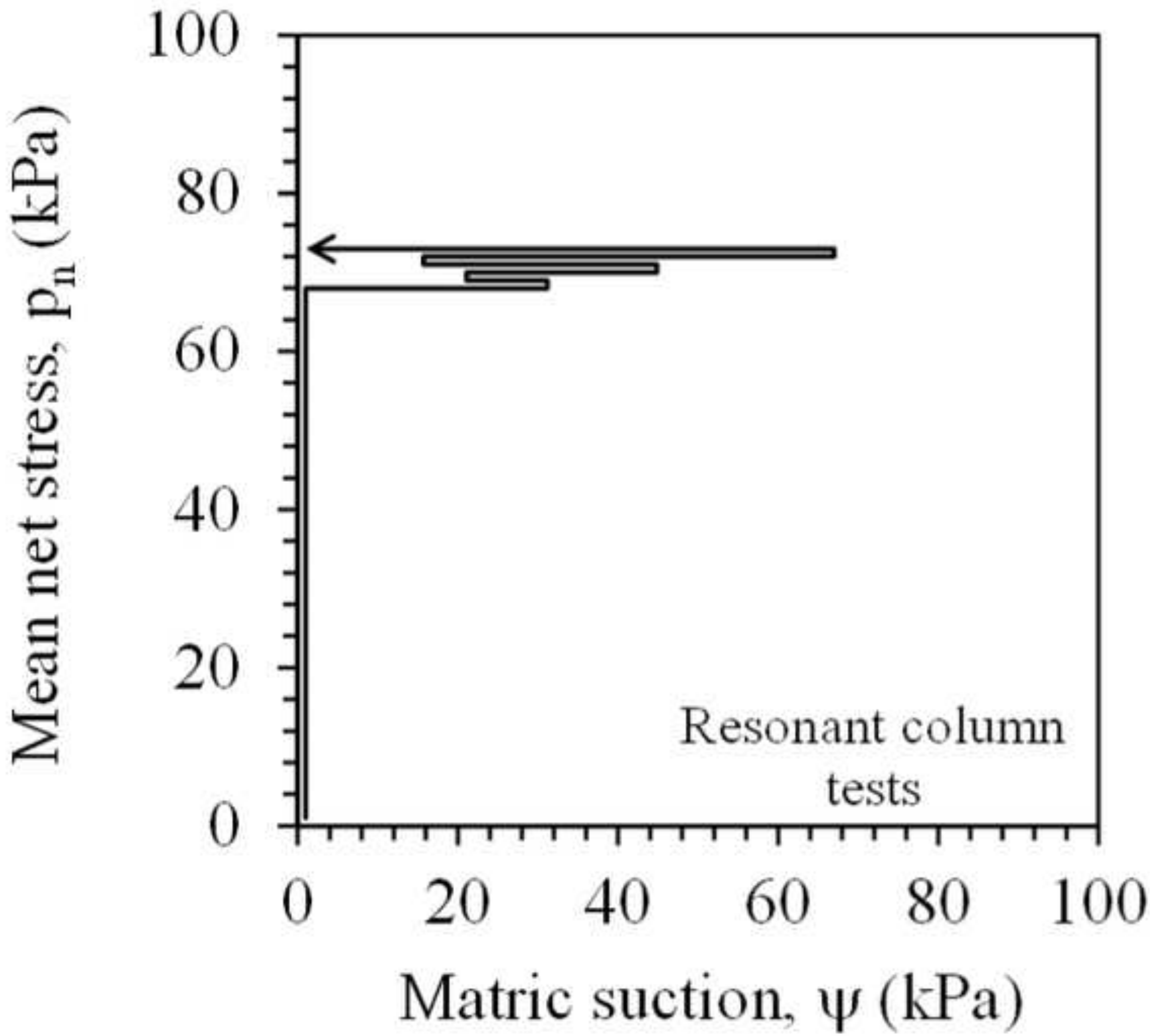

Figure 8
Click here to download high resolution image

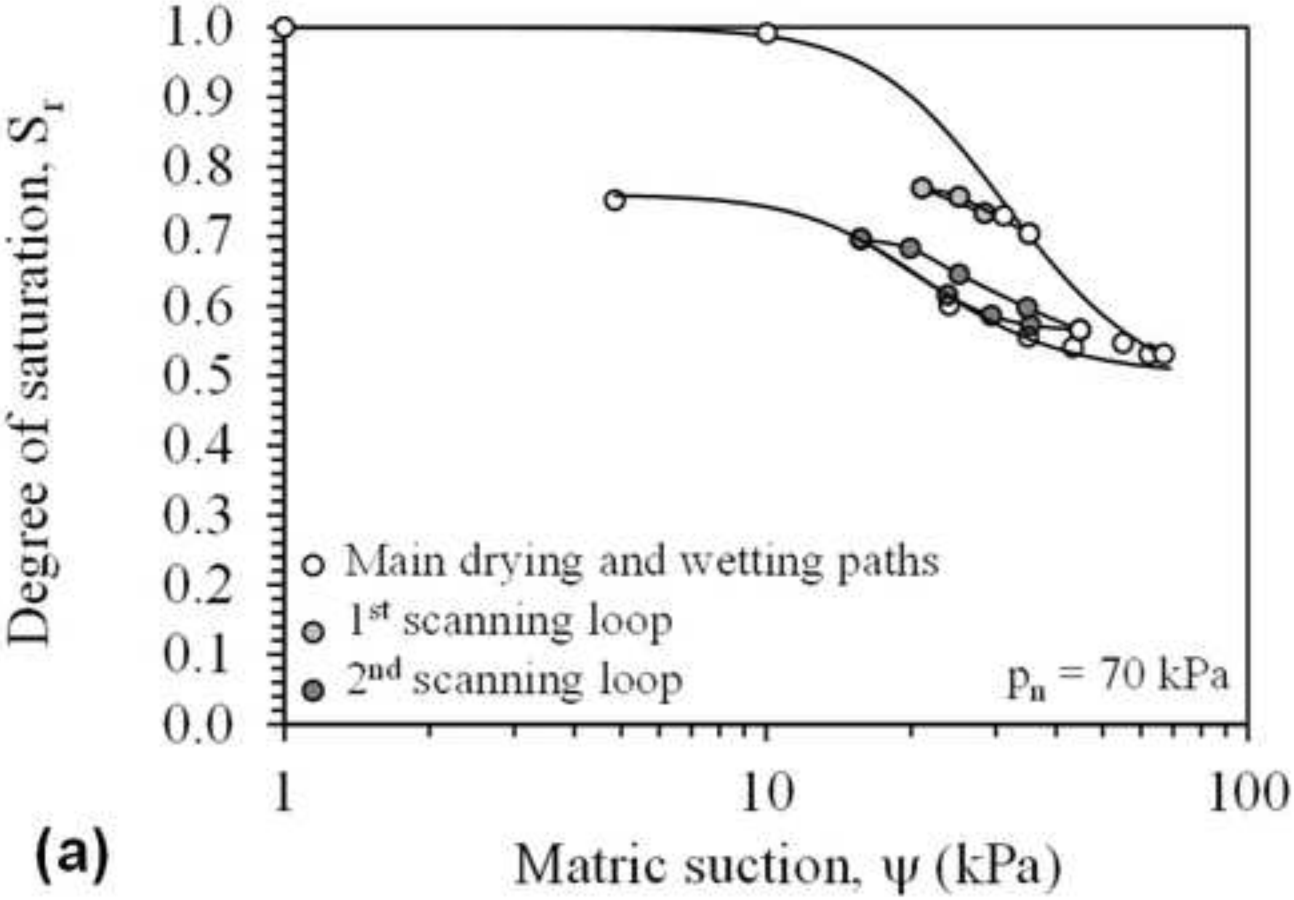

(a)

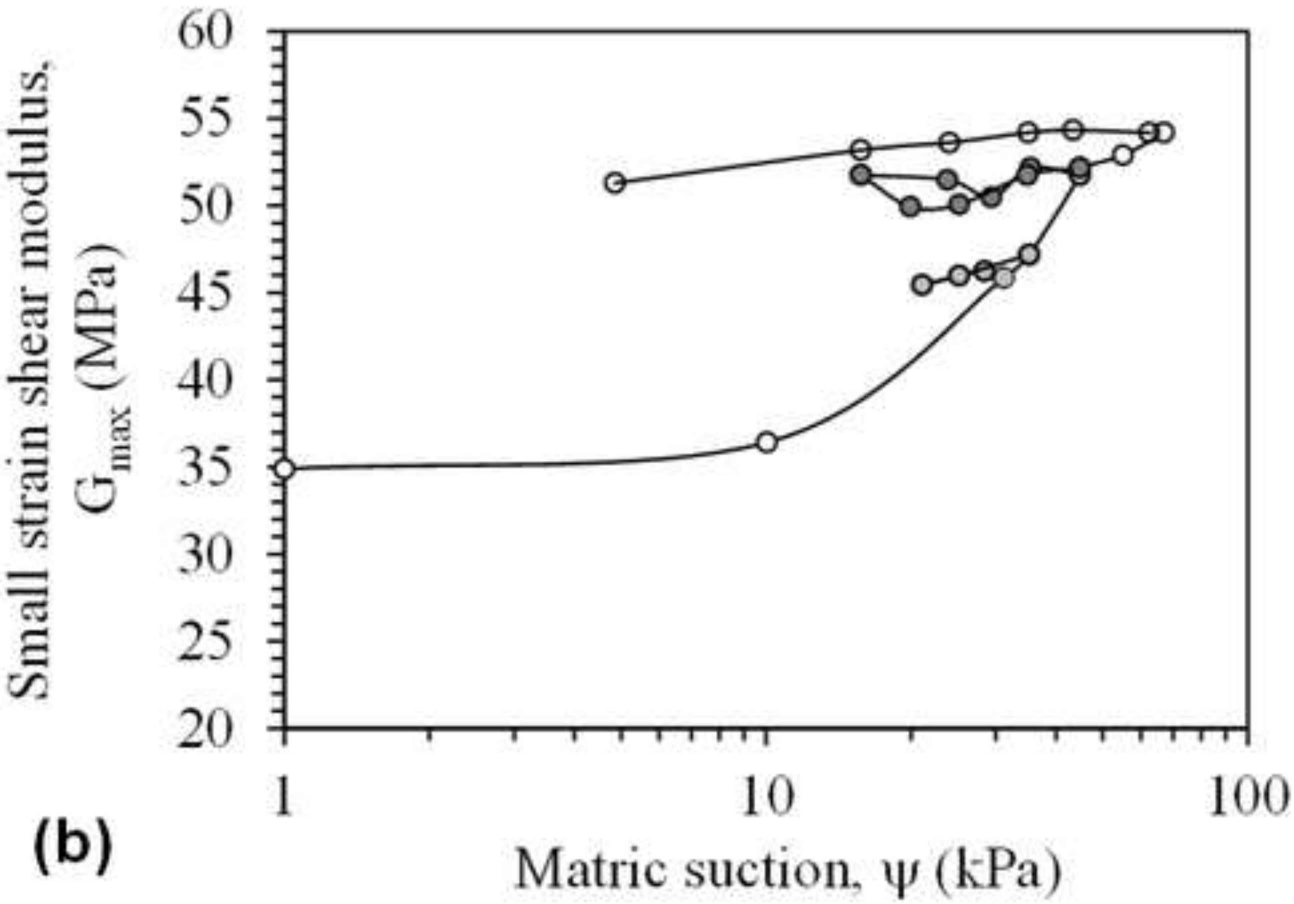

(b)

Figure 9

Click here to download high resolution image

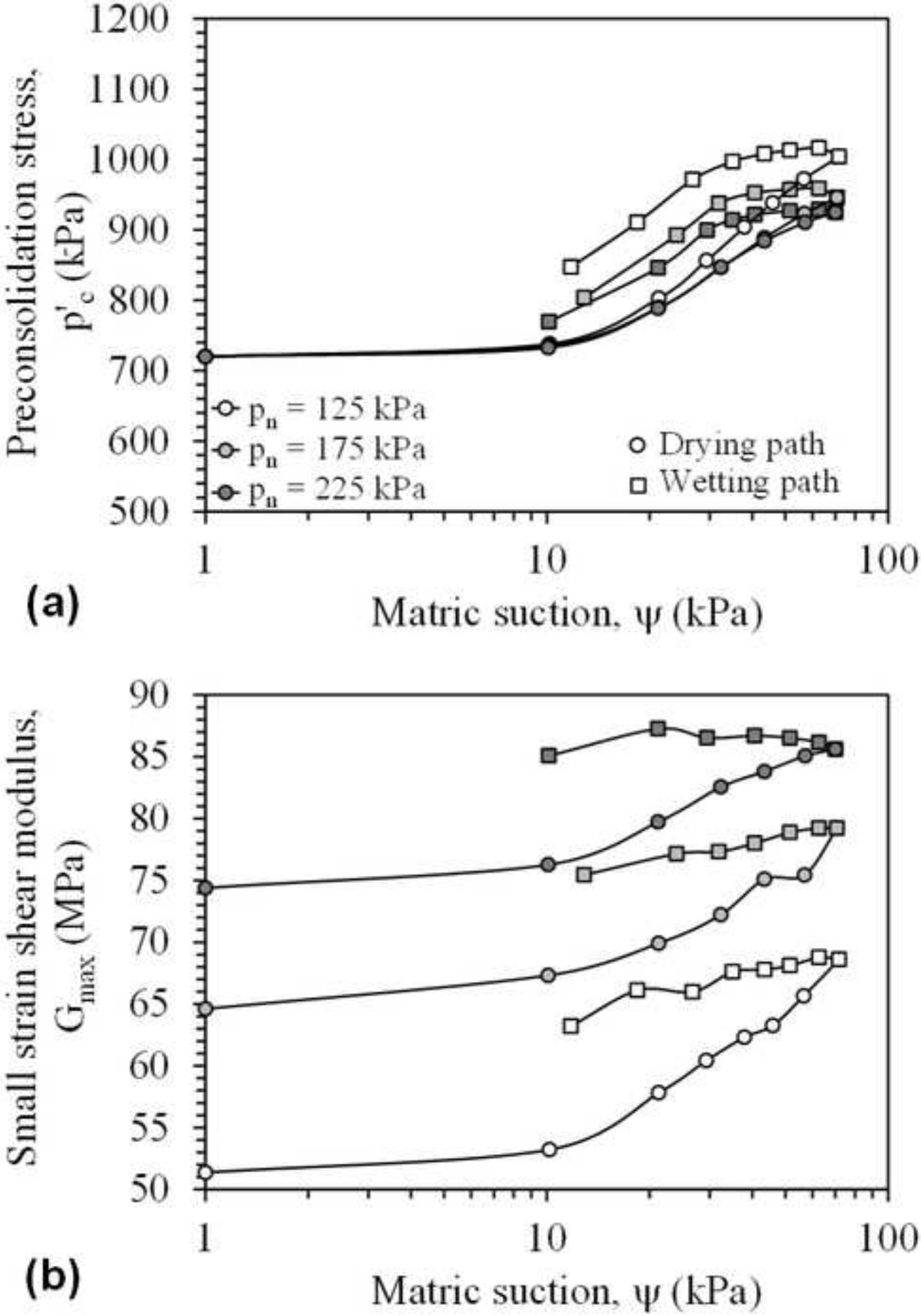

Figure 10
Click here to download high resolution image